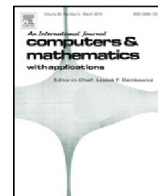




Contents lists available at ScienceDirect

Computers and Mathematics with Applications

journal homepage: www.elsevier.com/locate/camwa

Near conserving energy numerical schemes for two-dimensional coupled seismic wave equations

A.M. Portillo

IMUVA, Departamento de Matemática Aplicada, Escuela de Ingenierías Industriales, Universidad de Valladolid, Spain

ARTICLE INFO

Article history:

Received 26 May 2017

Received in revised form 15 September 2017

Accepted 28 October 2017

Available online xxx

Keywords:

Seismic wave equations

Energy

Finite differences

Splitting method

Geometric method

ABSTRACT

Two-dimensional coupled seismic waves, satisfying the equations of linear isotropic elasticity, on a rectangular domain with initial conditions and periodic boundary conditions, are considered. A quantity conserved by the solution of the continuous problem is used to check the numerical solution of the problem. Second order spatial derivatives, in the x direction, in the y direction and mixed derivative, are approximated by finite differences on a uniform grid. The ordinary second order in time system obtained is transformed into a first order in time system in the displacement and velocity vectors. For the time integration of this system, second order and fourth order exponential splitting methods, which are geometric integrators, are proposed. These explicit splitting methods are not unconditionally stable and the stability condition for time step and space step ratio is deduced. Numerical experiments displaying the good behavior in the long time integration and the efficiency of the numerical solution are provided.

© 2017 Elsevier Ltd. All rights reserved.

1. Introduction

Seismic waves are vibrations that travel through the Earth taking the energy released during earthquakes or by means of artificial sources such as chemical explosions, surface vibrators or weight-dropping devices. Geologists study seismic waves to find out the layers of the Earth, how thick they are as well as what composition and features they have. Seismic wave research also allows to predict earthquakes and tsunamis. In addition there are many engineering applications such as prospecting for oil deposits and locating subsurface water.

The equation of motion and Hooke's law, together with the initial and boundary conditions, fully characterize a problem of seismic wave propagation and motion. In seismic profiling, two dimensional (2D) seismic waves are often used for regional surveys. It is usual to approximate the problem as if the seismic waves satisfy the equations of linear isotropic elasticity. The equations of motion for a perfectly elastic, homogeneous, isotropic medium in 2D are [1]

$$\begin{cases} \partial_{tt} u_1 = \alpha_{11} \partial_{xx} u_1 + \alpha_{22} \partial_{yy} u_1 + 2\alpha_{12} \partial_{xy} u_2, \\ \partial_{tt} u_2 = \alpha_{22} \partial_{xx} u_2 + \alpha_{11} \partial_{yy} u_2 + 2\alpha_{12} \partial_{xy} u_1, \end{cases} \quad (1)$$

for the coefficients

$$\alpha_{11} = \frac{\lambda + 2\mu}{\rho}, \quad \alpha_{22} = \frac{\mu}{\rho}, \quad \alpha_{12} = \frac{\lambda + \mu}{2\rho}, \quad (2)$$

where ρ is the density of the material through which the waves propagate, λ is the first Lamé coefficient and μ is the modulus of rigidity or the second Lamé coefficient. These three parameters are spatial constants in homogeneous medium. From

E-mail address: anapor@mat.uva.es.<https://doi.org/10.1016/j.camwa.2017.10.032>

0898-1221/© 2017 Elsevier Ltd. All rights reserved.

Proposition 3.13 in [2], if the elasticity tensor is pointwise stable and strongly elliptic, then

$$\alpha_{11} > 0, \alpha_{22} > 0, \alpha_{12} > 0. \quad (3)$$

When we consider wave propagation on a plane, which is perpendicular to the y axis, the waves described by the displacement vector in the vertical x - z plane, are called P-SV waves. P waves propagate in a longitudinal mode with velocity $v_p = \sqrt{(\lambda + 2\mu)/\rho}$ and are the first waves from an earthquake to arrive at a seismograph. While S waves (in the vertical plane SV waves) move perpendicular to the direction of wave propagation, with velocity $v_s = \sqrt{\mu/\rho}$ and are the second waves to arrive at a seismograph. The elastodynamic equations of such P-SV waves are equal to the equations in (1). In the geophysical literature, second order in time equations. (1) have been solved using different formulations. So in [3], the equations for the P-SV wave are transformed into a first order in time system in the velocity vector of two components and the stress tensor of three components, in which equations involve only first order spatial derivatives. Then, derivatives are discretized by using second order centered finite differences. Later, the accuracy of this scheme was improved in [4] by using fourth-order differences in space. Another formulation of P-SV wave is presented in [5], where the wave equations are separated in two sets of equations involving only first-order spatial derivatives: one for the displacement fields and the other for potential fields. Four equations are used, which are one less than velocity-stress formulation considered in [3]. A dynamic seismic rupture simulation is performed in [6], using staggered-grid finite differences for a two-dimensional velocity-stress formulation similar to the one used in [3]. In our work, second order spatial derivatives in (1) are discretized by using second and fourth order finite differences and, the resulting second order in time ordinary system, is transformed into a first order in time system, in the displacement and velocity vectors.

We are interested in obtaining efficient high order in space and time schemes for the numerical solution of equations (1), with periodic boundary conditions (4)–(7) and initial conditions (8). As we have said, we approximate the spatial derivatives by finite differences and, as the boundary conditions are periodic, the matrix in the achieved ODEs system is formed by block circulant matrices in which each block is too a circulant matrix, which allows us to extract information about its eigenvalues. We prove that the matrix of the system is symmetric with non positive eigenvalues and moreover we locate the interval that contains such eigenvalues. We study well-posedness by using the discrete energy associated to the problem.

We rewrite the second order in time semi-discrete problem as first order in time and the resulting system turns out to be a Hamiltonian problem. This makes interesting to use geometric time integrators in its numerical solution. The system is split into two intermediate problems which are solved exactly. Second and fourth order splitting schemes are achieved by the flow composition of the two intermediate problems chosen. The stability condition for the ratio between the time step and the space step is studied in terms of the coefficients α_{11} and α_{22} .

Useful overviews of splitting methods can be found in the review papers [7–9]. Splitting schemes are especially useful in the scope of geometric integration. Actually, splitting integrators preserve structural properties of the original problem's flow as long as the intermediate problems' flow do. Geometric methods do, in general, nearly preserve the energy, i.e. a modified energy is preserved up to an exponentially small error term, or there is a spatially discrete energy conservation law [10]. The good performance of the geometric integrators in the long time integration of Hamiltonian ODEs systems is well showed in [11,12].

Many numerical schemes for Hamiltonian PDEs have been developed. In the present work we consider symplectic finite difference methods. Methods which not depend on mesh generation as meshless symplectic algorithms with radial basis functions interpolation are proposed for example in [13,14].

Although in the current paper we have focused on periodic boundary conditions, other interesting problems may need to consider artificial boundary conditions. We leave for future work to study if the proposed methods can handle for example absorbing boundary conditions, as we did in [15] with similar splitting methods, for the Klein–Gordon equation with Hagstrom–Warburton absorbing boundary conditions.

The paper is organized as follows. The energy of the continuous problem is introduced in Section 2. In Section 3, second and fourth order approximations of the spatial derivatives are considered and the corresponding discrete energies are regarded. The well-posedness of the semi discrete problems is deduced. Section 4 is devoted to the exponential splitting time integrators. Numerical experiments are conducted in Section 5. The good long time behavior as well as the efficiency of the splitting schemes by comparing with the fourth-order four-stage Runge–Kutta method in terms of CPU time are studied.

2. A conserved quantity of the continuous problem

In this work, we consider the two coupled wave equations in 2D (1), in a rectangular domain $R = [a, b] \times [c, d]$, for the unknowns $u_1(x, y, t)$ and $u_2(x, y, t)$ with periodic boundary conditions,

$$u_n(a, y, t) = u_n(b, y, t), \quad y \in [c, d], \quad (4)$$

$$\partial_x u_n(a, y, t) = \partial_x u_n(b, y, t), \quad y \in [c, d], \quad (5)$$

$$u_n(x, c, t) = u_n(x, d, t), \quad x \in [a, b], \quad (6)$$

$$\partial_y u_n(x, c, t) = \partial_y u_n(x, d, t), \quad x \in [a, b], \quad (7)$$

for $n = 1, 2$, and the initial conditions,

$$u_1(x, y, 0) = u_0(x, y), \quad \partial_t u_1(x, y, 0) = v_0(x, y), \tag{8}$$

$$u_2(x, y, 0) = w_0(x, y), \quad \partial_t u_2(x, y, 0) = z_0(x, y), \tag{9}$$

which satisfy periodic boundary conditions in R .

In general, the exact solution of this problem is not known and a numerical approximation is sought. Knowing a quantity conserved by the solution of the continuous problem can be useful as a reference for checking the numerical solution of the problem. Moreover, if this conserved quantity is also transferred to the semi-discrete in space problem, we can take advantage of geometric time integrators that almost retain this quantity.

We consider

$$\begin{aligned} E(t) &= \frac{1}{2} \iint_R ((\partial_t u_1(x, y, t))^2 + \alpha_{11}(\partial_x u_1(x, y, t))^2 + \alpha_{22}(\partial_y u_1(x, y, t))^2) dx dy \\ &+ \frac{1}{2} \iint_R ((\partial_t u_2(x, y, t))^2 + \alpha_{22}(\partial_x u_2(x, y, t))^2 + \alpha_{11}(\partial_y u_2(x, y, t))^2) dx dy \\ &+ \frac{1}{2} \iint_R 2\alpha_{12}(\partial_x u_1(x, y, t)\partial_y u_2(x, y, t) + \partial_y u_1(x, y, t)\partial_x u_2(x, y, t)) dx dy. \end{aligned} \tag{10}$$

It can be shown that solutions of (1) with periodic boundary conditions or homogeneous Dirichlet boundary conditions conserve $E(t)$. This can be done as follows. Multiplying the equations in (1) by $\partial_t u_1$ and $\partial_t u_2$ respectively, and adding both equations, the result can be rewritten as a divergence. Then, considering the integral over the rectangle R , it can be seen that $E'(t) = 0$, from the divergence theorem. Therefore $E(t)$ is constant with time and

$$\begin{aligned} E(t) = E(0) &= \frac{1}{2} \iint_R (v_0(x, y)^2 + \alpha_{11}(\partial_x u_0(x, y))^2 + \alpha_{22}(\partial_y u_0(x, y))^2) dx dy \\ &+ \frac{1}{2} \iint_R (z_0(x, y)^2 + \alpha_{22}(\partial_x w_0(x, y))^2 + \alpha_{11}(\partial_y w_0(x, y))^2) dx dy \\ &+ \iint_R \alpha_{12}(\partial_x u_0(x, y)\partial_y w_0(x, y) + \partial_y u_0(x, y)\partial_x w_0(x, y)) dx dy. \end{aligned} \tag{11}$$

In this way, we can compute the conserved quantity of the problem through the initial conditions.

3. Spatial discretization

We start approximating the spatial derivatives in (1) by using finite differences. For the sake of simplicity, we consider the same size step in both directions x and y , that is, for a value of N , $h = \frac{b-a}{N}$ and $M = \frac{d-c}{h}$. Let $x_j = a + (j - 1)h$, $j = 1, \dots, N + 1$, and $y_l = c + (l - 1)h$, $l = 1, \dots, M + 1$, be the nodes of the spatial discretization. This produces a uniform grid in the computational domain and a matrix of unknowns $u_{jl}(t) = u(x_j, y_l, t)$.

In general, finite difference approximation involves a stencil of points surrounding u_{jl} . For $n = 1, 2$, let it be $\mathbf{u}_{n,j}$ the approximations to the unknowns for fixed x_j , $(u_n(x_j, y_1), \dots, u_n(x_j, y_{M+1}))^T$. Denoting the vectors $\mathbf{u}_{1,h} = [\mathbf{u}_{1,1}^T, \dots, \mathbf{u}_{1,N+1}^T]^T$ and $\mathbf{u}_{2,h} = [\mathbf{u}_{2,1}^T, \dots, \mathbf{u}_{2,N+1}^T]^T$, we stretch each matrix of unknowns in a vector and we achieve the second order in time ODEs system

$$\frac{d^2}{dt^2} \begin{bmatrix} \mathbf{u}_{1,h} \\ \mathbf{u}_{2,h} \end{bmatrix} = A \begin{bmatrix} \mathbf{u}_{1,h} \\ \mathbf{u}_{2,h} \end{bmatrix}, \tag{12}$$

where A is a matrix of dimension $2(N + 1)(M + 1)$.

3.1. Second order spatial discretization

In this subsection, second order spatial derivatives in the direction x and in the direction y are approximated by second order central finite differences

$$\begin{aligned} \partial_{xx} u_{jl} &\approx \frac{u_{j-1,l} - 2u_{jl} + u_{j+1,l}}{h^2}, \\ \partial_{yy} u_{jl} &\approx \frac{u_{j,l-1} - 2u_{jl} + u_{j,l+1}}{h^2}, \end{aligned}$$

in stencil form,

$$\frac{1}{h^2} \begin{pmatrix} 0 & 0 & 0 \\ 1 & -2 & 1 \\ 0 & 0 & 0 \end{pmatrix}, \quad \frac{1}{h^2} \begin{pmatrix} 0 & 1 & 0 \\ 0 & -2 & 0 \\ 0 & 1 & 0 \end{pmatrix},$$

respectively.

are the diagonal matrices with eigenvalues

$$\lambda_{lk} = -2(\alpha_{11} + \alpha_{22}) + 2\alpha_{11} \cos\left(\frac{2\pi l}{N+1}\right) + 2\alpha_{22} \cos\left(\frac{2\pi k}{M+1}\right), \tag{18}$$

$$\mu_{lk} = -2\alpha_{12} \sin\left(\frac{2\pi l}{N+1}\right) \sin\left(\frac{2\pi k}{M+1}\right), \tag{19}$$

$$\tilde{\lambda}_{lk} = -2(\alpha_{11} + \alpha_{22}) + 2\alpha_{22} \cos\left(\frac{2\pi l}{N+1}\right) + 2\alpha_{11} \cos\left(\frac{2\pi k}{M+1}\right). \tag{20}$$

Proof. Denoting \otimes the Kronecker product of matrices, the matrix of eigenvectors is

$$P = V_{M+1} \otimes V_{N+1}, \tag{21}$$

being

$$V_{M+1} = \begin{bmatrix} 1 & 1 & \dots & 1 \\ \tilde{\omega}_1 & \tilde{\omega}_2 & \dots & \tilde{\omega}_{M+1} \\ \vdots & \vdots & & \vdots \\ \tilde{\omega}_1^M & \tilde{\omega}_2^M & \dots & \tilde{\omega}_{M+1}^M \end{bmatrix}, \quad V_{N+1} = \begin{bmatrix} 1 & 1 & \dots & 1 \\ \tilde{\varepsilon}_1 & \tilde{\varepsilon}_2 & \dots & \tilde{\varepsilon}_{N+1} \\ \vdots & \vdots & & \vdots \\ \tilde{\varepsilon}_1^N & \tilde{\varepsilon}_2^N & \dots & \tilde{\varepsilon}_{N+1}^N \end{bmatrix},$$

where

$$\tilde{\omega}_k = (\omega_{M+1})^k, \quad \omega_{M+1} = \exp\left(\frac{2\pi i}{M+1}\right),$$

$$\tilde{\varepsilon}_l = (\varepsilon_{N+1})^l, \quad \varepsilon_{N+1} = \exp\left(\frac{2\pi i}{N+1}\right).$$

We begin considering the matrix A_1 .

$$A_1 = \text{circ}(B_1, B_2, 0, \dots, 0, B_2),$$

$$B_1 = \text{circ}(-2(\alpha_{11} + \alpha_{22}), \alpha_{22}, 0, \dots, 0, \alpha_{22}),$$

$$B_2 = \text{circ}(\alpha_{11}, 0, \dots, 0).$$

We look at the following polynomials associated to the blocks of matrix A_1 ,

$$h_1(z) = -2(\alpha_{11} + \alpha_{22}) + \alpha_{22}z + \alpha_{22}z^M,$$

$$h_2(z) = \alpha_{11},$$

$$h_{N+1}(z) = \alpha_{11}.$$

Then, the eigenvalues of matrix A_1 are (see [16,17])

$$\lambda_{l,k} = \tilde{\varepsilon}_l^0 h_1(\tilde{\omega}_k) + \tilde{\varepsilon}_l h_2(\tilde{\omega}_k) + \tilde{\varepsilon}_l^N h_{N+1}(\tilde{\omega}_k), \quad l = 1, \dots, N+1, \quad k = 1, \dots, M+1,$$

and the eigenvectors are the columns of matrix P . Then,

$$\lambda_{l,k} = -2(\alpha_{11} + \alpha_{22}) + \alpha_{22} \left(\exp\left(\frac{2\pi ik}{M+1}\right) + \exp\left(\frac{2\pi ikM}{M+1}\right) \right) + \alpha_{11} \left(\exp\left(\frac{2\pi il}{N+1}\right) + \exp\left(\frac{2\pi ilN}{N+1}\right) \right).$$

Taking into account that,

$$\exp\left(\frac{2\pi ilN}{N+1}\right) = \exp\left(\frac{-2\pi il}{N+1}\right), \quad \exp\left(\frac{2\pi ikM}{M+1}\right) = \exp\left(\frac{-2\pi ik}{M+1}\right),$$

$$\lambda_{l,k} = -2(\alpha_{11} + \alpha_{22}) + 2\alpha_{11} \cos\left(\frac{2\pi l}{N+1}\right) + 2\alpha_{22} \cos\left(\frac{2\pi k}{M+1}\right).$$

A similar result can be obtained for matrix A_3 changing the roles of α_{11} and α_{22} , that is

$$\tilde{\lambda}_{l,k} = -2(\alpha_{11} + \alpha_{22}) + 2\alpha_{22} \cos\left(\frac{2\pi l}{N+1}\right) + 2\alpha_{11} \cos\left(\frac{2\pi k}{M+1}\right).$$

Finally,

$$\begin{aligned} A_2 &= \text{circ}(0, C_2, 0, \dots, 0, C_2^T), \\ C_2 &= \text{circ}(0, \frac{1}{2}\alpha_{12}, 0, \dots, 0, -\frac{1}{2}\alpha_{12}), \\ C_2^T &= \text{circ}(0, -\frac{1}{2}\alpha_{12}, 0, \dots, 0, \frac{1}{2}\alpha_{12}). \end{aligned}$$

We consider now the polynomials associated to the blocks of matrix A_2 ,

$$\begin{aligned} h_2(z) &= \frac{1}{2}\alpha_{12}(z - z^M), \\ h_{N+1}(z) &= -h_2(z). \end{aligned}$$

Then, the eigenvalues of matrix A_2 are (see [16,17])

$$\mu_{l,k} = \tilde{\epsilon}_l h_2(\tilde{\omega}_k) + \tilde{\epsilon}_l^N h_{N+1}(\tilde{\omega}_k), \quad l = 1, \dots, N + 1, \quad k = 1, \dots, M + 1,$$

and the eigenvectors are the columns of matrix P . That means

$$\begin{aligned} \mu_{l,k} &= \frac{1}{2}\alpha_{12}(\exp(\frac{2\pi ik}{M+1}) - \exp(\frac{2\pi ikM}{M+1}))(\exp(\frac{2\pi il}{N+1}) - \exp(\frac{2\pi ilN}{N+1})) \\ &= 2\alpha_{12} \sin(\frac{2\pi l}{N+1}) \sin(\frac{2\pi k}{M+1}). \quad \square \end{aligned}$$

Lemma 2. The eigenvalues of matrix A in (14), for the coefficients α_{ij} meeting (3) and

$$\alpha_{11}\alpha_{22} > \alpha_{12}^2, \tag{22}$$

satisfy

$$\sigma(A) \subset [\frac{-4(\alpha_{11} + \alpha_{22})}{h^2}, 0]. \tag{23}$$

Proof. From Lemma 1,

$$\begin{aligned} \begin{bmatrix} A_1 & A_2 \\ A_2 & A_3 \end{bmatrix} &= \begin{bmatrix} P^{-1}D_1P & P^{-1}D_2P \\ P^{-1}D_2P & P^{-1}D_3P \end{bmatrix} \\ &= \begin{bmatrix} P^{-1} & 0 \\ 0 & P^{-1} \end{bmatrix} \begin{bmatrix} D_1 & D_2 \\ D_2 & D_3 \end{bmatrix} \begin{bmatrix} P & 0 \\ 0 & P \end{bmatrix} \\ &= \begin{bmatrix} P & 0 \\ 0 & P \end{bmatrix}^{-1} \begin{bmatrix} D_1 & D_2 \\ D_2 & D_3 \end{bmatrix} \begin{bmatrix} P & 0 \\ 0 & P \end{bmatrix}. \end{aligned}$$

Then, the eigenvalues of matrix $\begin{bmatrix} A_1 & A_2 \\ A_2 & A_3 \end{bmatrix}$ are the same as the eigenvalues of matrix $D = \begin{bmatrix} D_1 & D_2 \\ D_2 & D_3 \end{bmatrix}$.

From formulas (18)–(20), it is plain that $\lambda_{lk} \leq 0, \tilde{\lambda}_{lk} \leq 0$, and $\mu_{lk} \in [-2\alpha_{12}, 2\alpha_{12}]$ for $l = 1, \dots, N + 1, k = 1, \dots, M + 1$. Moreover, $\lambda_{N+1,M+1} = \tilde{\lambda}_{N+1,M+1} = \mu_{N+1,M+1} = 0$, and $\lambda_{lk} < 0, \tilde{\lambda}_{lk} < 0$ for $l = 1, \dots, N, k = 1, \dots, M$. On the other hand, matrix D is symmetric and then its eigenvalues are real numbers. From Gershgorin's Theorem, every eigenvalue of D lies within at least one of the disks $D(\lambda_{lk}, |\mu_{lk}|)$ or $D(\tilde{\lambda}_{lk}, |\mu_{lk}|)$, for $l = 1, \dots, N + 1, k = 1, \dots, M + 1$. Our objective now is to prove that for $l = 1, \dots, N + 1, k = 1, \dots, M + 1$,

$$-4(\alpha_{11} + \alpha_{22}) \leq \lambda_{lk} + |\mu_{lk}| \leq 0, \tag{24}$$

$$-4(\alpha_{11} + \alpha_{22}) \leq \tilde{\lambda}_{lk} + |\mu_{lk}| \leq 0. \tag{25}$$

We are going to calculate the absolute extrema of the continuous function

$$f(x, y) = -2(\alpha_{11} + \alpha_{22}) + 2\alpha_{11} \cos(x) + 2\alpha_{22} \cos(y) - 2\alpha_{12} \sin(x) \sin(y),$$

on the compact set $K = [0, 2\pi] \times [0, 2\pi]$. The Weierstrass's Theorem guarantees that the absolute maximum and the absolute minimum of $f(x, y)$ are reached in points of $[0, 2\pi] \times [0, 2\pi]$. First, we study the function at the boundary.

If $y \in [0, 2\pi]$,

$$f(0, y) = f(2\pi, y) = -2(\alpha_{11} + \alpha_{22}) + 2\alpha_{11} + 2\alpha_{22} \cos(y).$$

In that case, $-4\alpha_{22} \leq f(0, y) = f(2\pi, y) \leq 0$.

If $x \in [0, 2\pi]$,

$$f(x, 0) = f(x, 2\pi) = -2(\alpha_{11} + \alpha_{22}) + 2\alpha_{11} \cos(x) + 2\alpha_{22}.$$

Thus, $-4\alpha_{11} \leq f(x, 0) = f(x, 2\pi) \leq 0$.

Second, we look for the possible extrema of $f(x, y)$ in $(0, 2\pi) \times (0, 2\pi)$, which have to satisfy

$$\frac{\partial f}{\partial x} = -2\alpha_{11} \sin(x) - 2\alpha_{12} \cos(x) \sin(y) = 0, \tag{26}$$

$$\frac{\partial f}{\partial y} = -2\alpha_{22} \sin(y) - 2\alpha_{12} \sin(x) \cos(y) = 0. \tag{27}$$

If $\sin(x) = \sin(y) = 0$ (26) and (27) are satisfied and then the point (π, π) is a solution of (26)–(27). We evaluate the function f in this possible extremum, $f(\pi, \pi) = -4(\alpha_{11} + \alpha_{22})$. Other possible solution of (26)–(27) complies with $\sin(x) \neq 0$ and $\sin(y) \neq 0$. From (27), we obtain

$$\sin(y) = -\frac{\alpha_{12}}{\alpha_{22}} \sin(x) \cos(y). \tag{28}$$

Taking (28) into (26) we reach

$$-2\alpha_{11} \sin(x) + 2\frac{\alpha_{12}^2}{\alpha_{22}} \cos(x) \sin(x) \cos(y) = 0,$$

and multiplying by $\frac{\alpha_{22}}{\sin(x)}$ we achieve

$$\alpha_{11}\alpha_{22} = \alpha_{12}^2 \cos(x) \cos(y) \leq \alpha_{12}^2,$$

which contradicts (22). Consequently the only solution of (26) and (27) is (π, π) . Then, summarizing the absolute minimum of $f(x, y)$ in $[0, 2\pi] \times [0, 2\pi]$ is $-4(\alpha_{11} + \alpha_{22})$ and the absolute maximum is 0.

A similar conclusion can be obtained considering the function

$$\tilde{f}(x, y) = -2(\alpha_{11} + \alpha_{22}) + 2\alpha_{11} \cos(x) + 2\alpha_{22} \cos(y) + 2\alpha_{12} \sin(x) \sin(y).$$

Therefore (24)–(25) are satisfied and

$$\sigma(A) \subset \left[\frac{-4(\alpha_{11} + \alpha_{22})}{h^2}, 0 \right]. \quad \square$$

Lemma 3. The matrix A in (14), for the coefficients α_{ij} satisfying (3) and (22), is a symmetric negative semidefinite matrix.

Proof. As the matrices A_1, A_2 and A_3 in (15)–(17) are symmetric, this is also true for the matrix A . From Lemma 2 it is deduced that A is a symmetric negative semidefinite matrix. \square

Theorem 4. The discrete energy

$$E_h(t)(\mathbf{u}_1, \mathbf{u}_2, \mathbf{v}_1, \mathbf{v}_2) = \frac{h^2}{2}(\mathbf{v}_1^T \mathbf{v}_1 + \mathbf{v}_2^T \mathbf{v}_2 - \begin{bmatrix} \mathbf{u}_1 \\ \mathbf{u}_2 \end{bmatrix}^T A \begin{bmatrix} \mathbf{u}_1 \\ \mathbf{u}_2 \end{bmatrix}), \tag{29}$$

is conserved for $(\mathbf{u}_{1,h}, \mathbf{u}_{2,h}, \mathbf{du}_{1,h}/dt, \mathbf{du}_{2,h}/dt)$, being $(\mathbf{u}_{1,h}, \mathbf{u}_{2,h})$ the solution of (12) with the matrix A of (14).

Proof. From Lemma 3, (29) is a seminorm. If $(\mathbf{u}_{1,h}, \mathbf{u}_{2,h})$ is a solution of (12),

$$\begin{aligned} & \frac{dE_h}{dt}(t)(\mathbf{u}_{1,h}, \mathbf{u}_{2,h}, \mathbf{du}_{1,h}/dt, \mathbf{du}_{2,h}/dt) \\ &= h^2 \frac{d\mathbf{u}_{1,h}}{dt}^T \frac{d^2\mathbf{u}_{1,h}}{dt^2} + h^2 \frac{d\mathbf{u}_{2,h}}{dt}^T \frac{d^2\mathbf{u}_{2,h}}{dt^2} - h^2 \begin{bmatrix} \frac{d\mathbf{u}_{1,h}}{dt} \\ \frac{d\mathbf{u}_{2,h}}{dt} \end{bmatrix}^T A \begin{bmatrix} \mathbf{u}_{1,h} \\ \mathbf{u}_{2,h} \end{bmatrix} \\ &= h^2 \begin{bmatrix} \frac{d\mathbf{u}_{1,h}}{dt} \\ \frac{d\mathbf{u}_{2,h}}{dt} \end{bmatrix}^T \left(\frac{d^2}{dt^2} \begin{bmatrix} \mathbf{u}_{1,h} \\ \mathbf{u}_{2,h} \end{bmatrix} - A \begin{bmatrix} \mathbf{u}_{1,h} \\ \mathbf{u}_{2,h} \end{bmatrix} \right) = 0. \quad \square \end{aligned}$$

Then the discrete energy is conserved and the problem (12) with matrix A in (14), is well posed.

3.2. Fourth order spatial discretization

Computational cost becomes especially important when the number of equations in the system increases. In order to approach Eqs. (1) with periodic boundary conditions (4)–(7) and initial conditions (8), with higher accuracy, it is convenient to introduce finite differences with order greater than two. Like this, higher computational efficiency can be achieved. In this section we consider fourth order approximation of the spatial derivatives in a similar way as in Section 1.3.1 of [18] in Section 3.1 of [19] and in Section 5 of [20].

Second order spatial derivatives in the direction x and in the direction y are approximated by fourth order central finite differences

$$\begin{aligned} \partial_{xx} u_{jl} &\approx \frac{1}{h^2} \left(-\frac{1}{12} u_{j-2,l} + \frac{4}{3} u_{j-1,l} - \frac{5}{2} u_{jl} + \frac{4}{3} u_{j+1,l} - \frac{1}{12} u_{j+2,l} \right), \\ \partial_{yy} u_{jl} &\approx \frac{1}{h^2} \left(-\frac{1}{12} u_{j,l-2} + \frac{4}{3} u_{j,l-1} - \frac{5}{2} u_{jl} + \frac{4}{3} u_{j,l+1} - \frac{1}{12} u_{j,l+2} \right), \end{aligned}$$

in stencil form,

$$\frac{1}{12h^2} \begin{pmatrix} 0 & 0 & 0 & 0 & 0 \\ 0 & 0 & 0 & 0 & 0 \\ -1 & 16 & -30 & 16 & -1 \\ 0 & 0 & 0 & 0 & 0 \\ 0 & 0 & 0 & 0 & 0 \end{pmatrix}, \quad \frac{1}{12h^2} \begin{pmatrix} 0 & 0 & -1 & 0 & 0 \\ 0 & 0 & 16 & 0 & 0 \\ 0 & 0 & -30 & 0 & 0 \\ 0 & 0 & 16 & 0 & 0 \\ 0 & 0 & -1 & 0 & 0 \end{pmatrix},$$

respectively.

Mixed derivative are approximated by the following fourth order finite differences

$$\begin{aligned} \partial_{xy} u_{jl} &\approx \frac{1}{144h^2} \{ u_{j-2,l-2} - 8u_{j-2,l-1} + 8u_{j-2,l+1} - u_{j-2,l+2} \\ &\quad - 8u_{j-1,l-2} + 64u_{j-1,l-1} - 64u_{j-1,l+1} + 8u_{j-1,l+2} \\ &\quad + 8u_{j+1,l-2} - 64u_{j+1,l-1} + 64u_{j+1,l+1} - 8u_{j+1,l+2} \\ &\quad - u_{j+2,l-2} + 8u_{j+2,l-1} - 8u_{j+2,l+1} + u_{j+2,l+2} \}, \end{aligned}$$

in stencil form,

$$\frac{1}{144h^2} \begin{pmatrix} -1 & 8 & 0 & -8 & 1 \\ 8 & -64 & 0 & 64 & -8 \\ 0 & 0 & 0 & 0 & 0 \\ -8 & 64 & 0 & -64 & 8 \\ 1 & -8 & 0 & 8 & -1 \end{pmatrix}.$$

In this case, the matrix of the problem (12) is

$$A = \frac{1}{h^2} \begin{bmatrix} A_1 & A_2 \\ A_2 & A_3 \end{bmatrix}. \tag{30}$$

A_1, A_2 and A_3 are the following matrices of dimension $(N + 1)(M + 1)$

$$A_1 = \frac{1}{72} \begin{bmatrix} B_1 & B_2 & B_3 & & & & B_3 & B_2 \\ B_2 & B_1 & B_2 & B_3 & & & & B_3 \\ B_3 & B_2 & B_1 & B_2 & B_3 & & & \\ & & & \ddots & \ddots & \ddots & \ddots & \ddots \\ & & & & B_3 & B_2 & B_1 & B_2 & B_3 \\ B_3 & & & & & B_3 & B_2 & B_1 & B_2 \\ B_2 & B_3 & & & & & B_3 & B_2 & B_1 \end{bmatrix}, \tag{31}$$

$$A_3 = \frac{1}{72} \begin{bmatrix} \tilde{B}_1 & \tilde{B}_2 & \tilde{B}_3 & & & & \tilde{B}_3 & \tilde{B}_2 \\ \tilde{B}_2 & \tilde{B}_1 & \tilde{B}_2 & \tilde{B}_3 & & & & \tilde{B}_3 \\ \tilde{B}_3 & \tilde{B}_2 & \tilde{B}_1 & \tilde{B}_2 & \tilde{B}_3 & & & \\ & & & \ddots & \ddots & \ddots & \ddots & \ddots \\ & & & & \tilde{B}_3 & \tilde{B}_2 & \tilde{B}_1 & \tilde{B}_2 & \tilde{B}_3 \\ \tilde{B}_3 & & & & & \tilde{B}_3 & \tilde{B}_2 & \tilde{B}_1 & \tilde{B}_2 \\ \tilde{B}_2 & \tilde{B}_3 & & & & & \tilde{B}_3 & \tilde{B}_2 & \tilde{B}_1 \end{bmatrix}, \tag{32}$$

$$A_2 = \frac{\alpha_{12}}{72} \begin{bmatrix} 0 & 8C_2 & -C_2 & & -C_2^T & 8C_2^T \\ 8C_2^T & 0 & 8C_2 & -C_2 & & -C_2^T \\ -C_2^T & 8C_2^T & 0 & 8C_2 & -C_2 & \\ & & \ddots & \ddots & \ddots & \ddots \\ & & & -C_2^T & 8C_2^T & 0 & 8C_2 & -C_2 \\ -C_2 & & & -C_2^T & 8C_2^T & 0 & 8C_2 \\ 8C_2 & -C_2 & & & -C_2^T & 8C_2^T & 0 \end{bmatrix}, \tag{33}$$

$$C_1 = \begin{bmatrix} -180 & 96 & -6 & & -6 & 96 \\ 96 & -180 & 96 & -6 & & -6 \\ -6 & 96 & -180 & 96 & -6 & \\ & & \ddots & \ddots & \ddots & \\ -6 & & & -6 & 96 & -180 & 96 & -6 \\ 96 & -6 & & & -6 & 96 & -180 & 96 \end{bmatrix},$$

$$C_2 = \begin{bmatrix} 0 & 8 & -1 & & 1 & -8 \\ -8 & 0 & 8 & -1 & & 1 \\ 1 & -8 & 0 & 8 & -1 & \\ & & \ddots & \ddots & \ddots & \\ -1 & & & 1 & -8 & 0 & 8 & 1 \\ 8 & -1 & & & 1 & -8 & 0 \end{bmatrix},$$

$$B_1 = \alpha_{22}C_1 - 180\alpha_{11}I_{M+1}, \quad B_2 = 96\alpha_{11}I_{M+1}, \quad B_3 = -6\alpha_{11}I_{M+1}, \\ \tilde{B}_1 = \alpha_{11}C_1 - 180\alpha_{22}I_{M+1}, \quad \tilde{B}_2 = 96\alpha_{22}I_{M+1}, \quad \tilde{B}_3 = -6\alpha_{22}I_{M+1}.$$

Notice that A_1, A_2 and A_3 are symmetric matrices which are five block circulant matrices and, in turn, each block is a circulant matrix with at most five elements non zero in each row.

Lemma 5. Matrices A_1, A_2 and A_3 in (31)–(33) diagonalize in the same basis. Let P be the matrix of eigenvectors (21) such that

$$A_1 = P^{-1}D_1P, \quad A_2 = P^{-1}D_2P, \quad A_3 = P^{-1}D_3P.$$

Then

$$D_1 = \frac{1}{72} \text{diag}(\lambda_{lk} : l = 1, \dots, N + 1, k = 1, \dots, M + 1),$$

$$D_2 = \frac{1}{72} \text{diag}(\mu_{lk} : l = 1, \dots, N + 1, k = 1, \dots, M + 1),$$

$$D_3 = \frac{1}{72} \text{diag}(\tilde{\lambda}_{lk} : l = 1, \dots, N + 1, k = 1, \dots, M + 1),$$

are the diagonal matrices with eigenvalues

$$\lambda_{lk} = 4(\alpha_{11}(-45 + 48 \cos(\frac{2\pi l}{N+1}) - 3 \cos(\frac{4\pi l}{N+1})) + \alpha_{22}(-45 + 48 \cos(\frac{2\pi k}{N+1}) - 3 \cos(\frac{4\pi k}{N+1}))), \tag{34}$$

$$\mu_{lk} = 4\alpha_{12}(-64 \sin(\frac{2\pi l}{N+1}) \sin(\frac{2\pi k}{M+1}) - \sin(\frac{4\pi l}{N+1}) \sin(\frac{4\pi k}{M+1}) + 8 \sin(\frac{2\pi l}{N+1}) \sin(\frac{4\pi k}{M+1}) + 8 \sin(\frac{4\pi l}{N+1}) \sin(\frac{2\pi k}{M+1})), \tag{35}$$

$$\tilde{\lambda}_{lk} = 4(\alpha_{22}(-45 + 48 \cos(\frac{2\pi l}{N+1}) - 3 \cos(\frac{4\pi l}{N+1})) + \alpha_{11}(-45 + 48 \cos(\frac{2\pi k}{N+1}) - 3 \cos(\frac{4\pi k}{N+1}))). \tag{36}$$

Proof. We study first the matrix A_1 .

$$\begin{aligned} A_1 &= \text{circ}(B_1, B_2, B_3, 0, \dots, 0, B_3, B_2), \\ B_1 &= \text{circ}(-180(\alpha_{11} + \alpha_{22}), 96\alpha_{22}, -6\alpha_{22}, 0, \dots, 0, -6\alpha_{22}, 96\alpha_{22}), \\ B_2 &= \text{circ}(96\alpha_{11}, 0, \dots, 0), \\ B_3 &= \text{circ}(-6\alpha_{11}, 0, \dots, 0). \end{aligned}$$

We consider the following polynomials associated to the blocks of matrix A_1 ,

$$\begin{aligned} h_1(z) &= -180(\alpha_{11} + \alpha_{22}) + 96\alpha_{22}z - 6\alpha_{22}z^2 - 6\alpha_{22}z^{M-1} + 96\alpha_{22}z^M, \\ h_2(z) &= 96\alpha_{11}, \\ h_3(z) &= -6\alpha_{11}, \\ h_N(z) &= -6\alpha_{11}, \\ h_{N+1}(z) &= 96\alpha_{11}. \end{aligned}$$

Then, the eigenvalues of matrix A_1 are (see [16,17])

$$\begin{aligned} \lambda_{l,k} &= \tilde{\varepsilon}_l^0 h_1(\tilde{\omega}_k) + \tilde{\varepsilon}_l h_2(\tilde{\omega}_k) + \tilde{\varepsilon}_l^2 h_3(\tilde{\omega}_k) + \tilde{\varepsilon}_l^{N-1} h_N(\tilde{\omega}_k) + \tilde{\varepsilon}_l^N h_{N+1}(\tilde{\omega}_k), \\ l &= 1, \dots, N + 1, k = 1, \dots, M + 1, \end{aligned}$$

and the eigenvectors are the columns of matrix P . Then,

$$\begin{aligned} \lambda_{l,k} &= -180(\alpha_{11} + \alpha_{22}) + \alpha_{22}(96 \exp(\frac{2\pi ik}{M+1}) - 6 \exp(\frac{4\pi ik}{M+1}) \\ &\quad - 6 \exp(\frac{2\pi ik(M-1)}{M+1}) + 96 \exp(\frac{2\pi ikM}{M+1})) \\ &\quad + \alpha_{11}(96 \exp(\frac{2\pi ik}{M+1}) - 6 \exp(\frac{4\pi ik}{M+1}) \\ &\quad - 6 \exp(\frac{2\pi ik(M-1)}{M+1}) + 96 \exp(\frac{2\pi ikM}{M+1})). \end{aligned}$$

Taking into account that,

$$\exp(\frac{2\pi ilN}{N+1}) = \exp(\frac{-2\pi il}{N+1}), \quad \exp(\frac{2\pi il(N-1)}{N+1}) = \exp(\frac{-4\pi il}{N+1}),$$

$$\begin{aligned} \lambda_{l,k} &= -180(\alpha_{11} + \alpha_{22}) + \alpha_{11}(96 \cdot 2 \cos(\frac{2\pi l}{N+1}) - 6 \cdot 2 \cos(\frac{4\pi l}{N+1})) \\ &\quad + \alpha_{22}(96 \cdot 2 \cos(\frac{2\pi k}{M+1}) - 6 \cdot 2 \cos(\frac{4\pi k}{M+1})). \end{aligned}$$

A similar result can be obtained for matrix A_3 changing the roles of α_{11} and α_{22} .

Finally, we regard matrix A_2 .

$$\begin{aligned} A_2 &= \alpha_{12} \text{circ}(0, 8C_2, -C_2, 0, \dots, 0, -C_2^T, 8C_2^T), \\ C_2 &= \text{circ}(0, 8, -1, 0, \dots, 0, 1, -8), \\ C_2^T &= \text{circ}(0, -8, 1, 0, \dots, 0, -1, 8). \end{aligned}$$

We look upon the polynomials associated to the blocks of matrix A_2 ,

$$\begin{aligned} h_2(z) &= 64z - 8z^2 + 8z^{M-1} - 64z^M, \\ h_3(z) &= -8z + z^2 - z^{M-1} + 8z^M, \\ h_N(z) &= -h_3(z), \\ h_{N+1}(z) &= -h_2(z). \end{aligned}$$

Then, the eigenvalues of matrix A_2 are (see [16,17]) α_{12} times

$$\begin{aligned} \tilde{\varepsilon}_l h_2(\tilde{\omega}_k) + \tilde{\varepsilon}_l^2 h_3(\tilde{\omega}_k) + \tilde{\varepsilon}_l^{N-1} h_N(\tilde{\omega}_k) + \tilde{\varepsilon}_l^N h_{N+1}(\tilde{\omega}_k), \\ l = 1, \dots, N + 1, k = 1, \dots, M + 1, \end{aligned}$$

and the eigenvectors are the columns of matrix P . Working out,

$$\begin{aligned} & \exp\left(\frac{2\pi il}{N+1}\right)\left(64 \exp\left(\frac{2\pi ik}{M+1}\right) - 8 \exp\left(\frac{4\pi ik}{M+1}\right) + 8 \exp\left(\frac{2\pi ik(M-1)}{M+1}\right) - 64 \exp\left(\frac{2\pi ikM}{M+1}\right)\right) \\ & + \exp\left(\frac{4\pi il}{N+1}\right)\left(-8 \exp\left(\frac{2\pi ik}{M+1}\right) + \exp\left(\frac{4\pi ik}{M+1}\right) - \exp\left(\frac{2\pi ik(M-1)}{M+1}\right) + 8 \exp\left(\frac{2\pi ikM}{M+1}\right)\right) \\ & + \exp\left(\frac{2\pi il(N-1)}{N+1}\right)\left(8 \exp\left(\frac{2\pi ik}{M+1}\right) - \exp\left(\frac{4\pi ik}{M+1}\right) + \exp\left(\frac{2\pi ik(M-1)}{M+1}\right) - 8 \exp\left(\frac{2\pi ikM}{M+1}\right)\right) \\ & + \exp\left(\frac{2\pi ilN}{N+1}\right)\left(-64 \exp\left(\frac{2\pi ik}{M+1}\right) + 8 \exp\left(\frac{4\pi ik}{M+1}\right) - 8 \exp\left(\frac{2\pi ik(M-1)}{M+1}\right) + 64 \exp\left(\frac{2\pi ikM}{M+1}\right)\right). \end{aligned}$$

Therefore,

$$\begin{aligned} \mu_{l,k} = & 4\alpha_{12}\left(-64 \sin\left(\frac{2\pi l}{N+1}\right)\sin\left(\frac{2\pi k}{M+1}\right) + 8 \sin\left(\frac{2\pi l}{N+1}\right)\sin\left(\frac{4\pi k}{M+1}\right)\right. \\ & \left. + 8 \sin\left(\frac{4\pi l}{N+1}\right)\sin\left(\frac{2\pi k}{M+1}\right) - \sin\left(\frac{4\pi l}{N+1}\right)\sin\left(\frac{4\pi k}{M+1}\right)\right). \quad \square \end{aligned}$$

Lemma 6. The eigenvalues of matrix A in (30), for the coefficients α_{ij} meeting (3) and

$$\alpha_{11}\alpha_{22} > \frac{25}{9}\alpha_{12}, \tag{37}$$

satisfy

$$\sigma(A) \subset \left[\frac{-16(\alpha_{11} + \alpha_{22})}{3h^2}, 0 \right]. \tag{38}$$

Proof. From Lemma 5, the eigenvalues of matrix $\begin{bmatrix} A_1 & A_2 \\ A_2 & A_3 \end{bmatrix}$ are the same as the eigenvalues of matrix $D = \begin{bmatrix} D_1 & D_2 \\ D_2 & D_3 \end{bmatrix}$.

We consider the continuous function $g(x) = -15 + 16 \cos(x) - \cos(2x)$, $x \in [0, 2\pi]$. It is easy to see that

$$-32 = \min(g(0), g(\pi), g(2\pi)) \leq g(x) \leq \max(g(0), g(\pi), g(2\pi)) = 0. \tag{39}$$

From formulas (34), (36) and (39), we can deduce that $\lambda_{lk} \leq 0$, $\tilde{\lambda}_{lk} \leq 0$.

From (35), μ_{lk} can be rewritten as

$$\mu_{l,k} = -4\alpha_{12}\left(8 \sin\left(\frac{2\pi l}{N+1}\right) - \sin\left(\frac{4\pi l}{N+1}\right)\right)\left(8 \sin\left(\frac{2\pi k}{M+1}\right) - \sin\left(\frac{4\pi k}{M+1}\right)\right)$$

and $\mu_{lk} \in [-324\alpha_{12}, 324\alpha_{12}]$ for $l = 1, \dots, N+1, k = 1, \dots, M+1$. Moreover, $\lambda_{N+1,M+1} = \tilde{\lambda}_{N+1,M+1} = \mu_{N+1,M+1} = 0$, and $\lambda_{lk} < 0, \tilde{\lambda}_{lk} < 0$ for $l = 1, \dots, N, k = 1, \dots, M$. On the other hand, matrix D is symmetric and then its eigenvalues are real numbers. From Gershgorin's Theorem, every eigenvalue of D lies within at least one of the disks $D(\lambda_{lk}, |\mu_{lk}|)$ or $D(\tilde{\lambda}_{lk}, |\mu_{lk}|)$, for $l = 1, \dots, N+1, k = 1, \dots, M+1$. Our objective now is to prove that for $l = 1, \dots, N+1, k = 1, \dots, M+1$,

$$-4 \cdot 96(\alpha_{11} + \alpha_{22}) \leq \lambda_{lk} + |\mu_{lk}| \leq 0, \tag{40}$$

$$-4 \cdot 96(\alpha_{11} + \alpha_{22}) \leq \tilde{\lambda}_{lk} + |\mu_{lk}| \leq 0. \tag{41}$$

We are going to calculate the absolute extrema of the continuous function

$$\begin{aligned} f(x, y) = & \alpha_{11}(-45 + 48 \cos(x) - 3 \cos(2x)) + \alpha_{22}(-45 + 48 \cos(y) - 3 \cos(2y)) \\ & - \alpha_{12}(8 \sin(x) - \sin(2x))(8 \sin(y) - \sin(2y)), \end{aligned}$$

on the compact set $K = [0, 2\pi] \times [0, 2\pi]$. The Weierstrass's Theorem guarantees that the absolute maximum and the absolute minimum of $f(x, y)$ are reached in points of $[0, 2\pi] \times [0, 2\pi]$. First, we study the function at the boundary.

If $y \in [0, 2\pi]$,

$$\begin{aligned} f(0, y) = f(2\pi, y) = & \alpha_{22}(-45 + 48 \cos(y) - 3 \cos(2y)) \\ = & 3\alpha_{22}(-15 + 16 \cos(y) - \cos(2y)). \end{aligned}$$

In that case, from (39), $-96\alpha_{22} \leq f(0, y) = f(2\pi, y) \leq 0$.

If $x \in [0, 2\pi]$,

$$f(x, 0) = f(x, 2\pi) = \alpha_{11}(-45 + 48 \cos(x) - 3 \cos(2x)).$$

Thus, from (39), $-96\alpha_{11} \leq f(x, 0) = f(x, 2\pi) \leq 0$.

Second, we look for the possible extrema of $f(x, y)$ in $(0, 2\pi) \times (0, 2\pi)$, which have to satisfy

$$\frac{\partial f}{\partial x} = -6\alpha_{11}(8 \sin(x) - \sin(2x)) - \alpha_{12}(8 \cos(x) - 2 \cos(2x))(8 \sin(y) - \sin(2y)) = 0, \tag{42}$$

$$\frac{\partial f}{\partial y} = -6\alpha_{22}(8 \sin(y) - \sin(2y)) - \alpha_{12}(8 \cos(y) - 2 \cos(2y))(8 \sin(x) - \sin(2x)) = 0. \tag{43}$$

Taking into account that

$$8 \sin(x) - \sin(2x) = 0 \iff x = 0, \pi, 2\pi,$$

Eqs. (42) and (43) are satisfied if $x = y = \pi$, in which $f(\pi, \pi) = -96(\alpha_{11} + \alpha_{22})$, or if $8 \sin(x) - \sin(2x) \neq 0$ and $8 \sin(y) - \sin(2y) \neq 0$ when

$$\alpha_{11} = \frac{\alpha_{12}(-8 \cos(x) + 2 \cos(2x))}{6(8 \sin(x) - \sin(2x))}(8 \sin(y) - \sin(2y)), \tag{44}$$

$$\alpha_{22} = \frac{\alpha_{12}(-8 \cos(y) + 2 \cos(2y))}{6(8 \sin(y) - \sin(2y))}(8 \sin(x) - \sin(2x)). \tag{45}$$

From (44) and (45),

$$\alpha_{11}\alpha_{22} = \frac{\alpha_{12}^2}{6^2}(-8 \cos(x) + 2 \cos(2x))(-8 \cos(y) + 2 \cos(2y)) \leq \frac{\alpha_{12}^2}{6^2} 10^2, \tag{46}$$

which is incompatible with condition (37). Then, the only possible extremum in $(0, 2\pi) \times (0, 2\pi)$ is the point (π, π) . Then, the absolute minimum of $f(x, y)$ in $[0, 2\pi] \times [0, 2\pi]$ is $-96(\alpha_{11} + \alpha_{22})$ and the absolute maximum is 0.

A similar conclusion can be obtained considering the function

$$\begin{aligned} \tilde{f}(x, y) &= \alpha_{11}(-45 + 48 \cos(x) - 3 \cos(2x)) + \alpha_{22}(-45 + 48 \cos(y) - 3 \cos(2y)) \\ &\quad + \alpha_{12}(8 \sin(x) - \sin(2x))(8 \sin(y) - \sin(2y)). \end{aligned}$$

Therefore (40)–(41) are satisfied and

$$\sigma(A) \subset \left[\frac{-16(\alpha_{11} + \alpha_{22})}{3h^2}, 0 \right]. \quad \square$$

Lemma 7. The matrix A in (30), for the coefficients α_{ij} satisfying (3) and (37), is a symmetric negative semidefinite matrix.

Proof. As the matrices A_1, A_2 and A_3 in (31)–(33) are symmetric, this is also true for the matrix A . From Lemma 6 it is deduced that A is a symmetric negative semidefinite matrix. \square

Theorem 8. The discrete energy

$$E_h(t)(\mathbf{u}_1, \mathbf{u}_2, \mathbf{v}_1, \mathbf{v}_2) = \frac{h^2}{2}(\mathbf{v}_1^T \mathbf{v}_1 + \mathbf{v}_2^T \mathbf{v}_2 - \begin{bmatrix} \mathbf{u}_1 \\ \mathbf{u}_2 \end{bmatrix}^T A \begin{bmatrix} \mathbf{u}_1 \\ \mathbf{u}_2 \end{bmatrix}), \tag{47}$$

is conserved for $(\mathbf{u}_{1,h}, \mathbf{u}_{2,h}, \mathbf{d}\mathbf{u}_{1,h}/dt, \mathbf{d}\mathbf{u}_{2,h}/dt)$, being $(\mathbf{u}_{1,h}, \mathbf{u}_{2,h})$ the solution of (12) with the matrix A of (30).

Proof. The proof is similar to the one for Theorem 4. \square

Then the discrete energy is conserved and the problem (12) with the matrix A of (30), is well posed.

Remark 9. In Lemma 2, we have proved that conditions (3) and (22) on the coefficients α_{ij} are sufficient to comply with (23). Nevertheless we have seen numerically that (22) is not necessary and (23) holds too when the coefficients α_{ij} satisfy only (3).

Remark 10. In Lemma 6, we have proved that conditions (3) and (37) on the coefficients α_{ij} are sufficient to fulfill (38). However we have seen numerically that condition (37) can be weakened to (22) and (38) is still valid.

Remark 11. We have also seen numerically that if the coefficients α_{ij} meeting only (3), the eigenvalues of matrix A in (30) are less than or equal to zero. If condition (22) is not kept then $\sigma(A) \subset [\beta, 0]$ with $\beta < \frac{-16(\alpha_{11} + \alpha_{22})}{3h^2}$.

3.3. Typical values of elastic constants for layers of the earth

Lemma 2 and Lemma 6 work with conditions (3) and (22) on the coefficients α_{ij} , as we have commented in Remark 10. In this subsection we want to test if condition (22) is valid for the typical values of elastic constants of the Earth. For this, we

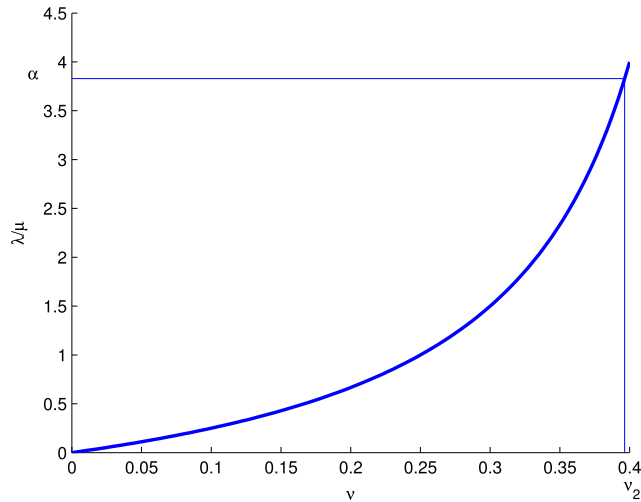


Fig. 1. λ/μ versus ν .

first rewrite (22) in terms of λ and μ . So, (22) is equivalent to

$$(\lambda + 2\mu)\mu - \left(\frac{\lambda + \mu}{2}\right)^2 > 0,$$

and dividing by μ^2 , we have

$$4\left(\frac{\lambda}{\mu} + 2\right) - \left(\frac{\lambda}{\mu} + 1\right)^2 > 0,$$

which is the same as

$$\left(\frac{\lambda}{\mu}\right)^2 - 2\frac{\lambda}{\mu} - 7 < 0.$$

This happens when

$$-1.8284 \approx 1 - 2\sqrt{2} < \frac{\lambda}{\mu} < 1 + 2\sqrt{2} = \alpha \approx 3.8284.$$

Then, we relate $\frac{\lambda}{\mu}$ to ν , the Poisson's ratio, which is a dimensionless value, by means of

$$\frac{\lambda}{\mu} = \frac{2\nu}{1 - 2\nu}.$$

We calculate the value ν which corresponds to the fixed value of $\lambda/\mu = \alpha$

$$\frac{2\nu}{1 - 2\nu} = \alpha$$

with the formula

$$\nu = \frac{\alpha}{2(1 + \alpha)}.$$

In this way, we obtain $\nu_2 \approx 0.3964$. In Fig. 1 is displayed $\frac{\lambda}{\mu}$ as a function of ν and the values α , ν_2 are indicated.

In Table F.1 of appendix F of [21], the values of ν for the different layers of the Earth are collected. It can be seen that $0.2549 \leq \nu \leq 0.3051$, without considering the core, in the rest of the layers, from a radius of 3800 km to a radius of 6368 km. Consequently, in view of Fig. 1 condition (22) is compatible with these layers of the Earth.

3.4. Approaching the continuous energy with the discrete energies

In this subsection we prove that the discrete energies considered in Theorem 4 in Section 3.1 and in Theorem 8 in Section 3.2 approach the continuous energy (10).

Lemma 12. Let $f(x, y) \in C^4(\mathbb{R})$ a function with compact support contained in an open set Ω such that $\Omega \subset \mathbb{R}$. Then

$$\iint_R f(x, y) dx dy - h^2 \sum_{j=1}^{N+1} \sum_{l=1}^{M+1} f(x_j, y_l) = O(h^4). \tag{48}$$

Proof. It is known that, if $g(x) \in C^4([x_j, x_{j+1}])$, there is $v_j \in (x_j, x_{j+1})$ such that the corrected trapezoidal rule

$$I_{CT}(g, [x_j, x_{j+1}]) = \frac{h}{2}(g(x_j) + g(x_{j+1})) + \frac{h^2}{12}(g'(x_j) - g'(x_{j+1})),$$

based on cubic Hermite interpolation of $g(x)$ and $g'(x)$ at x_j and x_{j+1} , satisfies

$$\int_{x_j}^{x_{j+1}} g(x) dx = I_{CT}(g, [x_j, x_{j+1}]) + \frac{h^5}{720} g^{(4)}(v_j).$$

Denoting $R_{jl} = [x_j, x_{j+1}] \times [y_l, y_{l+1}]$, to approach $\iint_{R_{jl}} f(x, y) dx dy$, we consider first the corrected trapezoidal rule in $\int_{x_j}^{x_{j+1}} f(x, y) dx$,

$$\begin{aligned} & \iint_{R_{jl}} f(x, y) dx dy \\ &= \int_{y_l}^{y_{l+1}} \left(\frac{h}{2}(f(x_j, y) + f(x_{j+1}, y)) + \frac{h^2}{12}(\partial_x f(x_j, y) - \partial_x f(x_{j+1}, y)) \right) dy \\ &+ \int_{y_l}^{y_{l+1}} \frac{h^5}{720} \partial_{xxxx} f(v_j, y) dy, \end{aligned}$$

and then, we apply again the corrected trapezoidal rule in the variable y . In this way we achieve the following rule

$$\begin{aligned} I_{CT2}(f, R_{jl}) &= \frac{h^2}{4}(f(x_j, y_l) + f(x_{j+1}, y_l) + f(x_j, y_{l+1}) + f(x_{j+1}, y_{l+1})) \\ &+ \frac{h^3}{24}(\partial_x f(x_j, y_l) - \partial_x f(x_{j+1}, y_l) + \partial_x f(x_j, y_{l+1}) - \partial_x f(x_{j+1}, y_{l+1})) \\ &+ \frac{h^3}{24}(\partial_y f(x_j, y_l) - \partial_y f(x_j, y_{l+1}) + \partial_y f(x_{j+1}, y_l) - \partial_y f(x_{j+1}, y_{l+1})) \\ &+ \frac{h^4}{144}(\partial_{xy} f(x_j, y_l) - \partial_{xy} f(x_j, y_{l+1}) + \partial_{xy} f(x_{j+1}, y_l) - \partial_{xy} f(x_{j+1}, y_{l+1})). \end{aligned}$$

The composite rule in R ,

$$I_{CT2}^C(f, R) = \sum_{j=1}^N \sum_{l=1}^M I_{CT2}(f, R_{jl}),$$

satisfies

$$\iint_R f(x, y) dx dy - I_{CT2}^C(f, R) = O(h^4).$$

Since $f(x, y)$ has compact support contained in an open set $\Omega \subset \mathbb{R}$,

$$I_{CT2}^C(f, R) = h^2 \sum_{j=1}^{N+1} \sum_{l=1}^{M+1} f(x_j, y_l)$$

and (48) is achieved. \square

Lemma 13. The continuous energy (10) can be rewritten as

$$\begin{aligned} E(t) &= \frac{1}{2} \iint_R (\partial_t u_1(x, y, t))^2 dx dy + \frac{1}{2} \iint_R (\partial_t u_2(x, y, t))^2 dx dy \\ &- \frac{1}{2} \iint_R (u_1 \partial_{tt} u_1(x, y, t) + u_2 \partial_{tt} u_2(x, y, t)) dx dy. \end{aligned} \tag{49}$$

Proof. Taking into account that

$$\begin{aligned} \partial_x(u_1 \partial_x u_1) &= \partial_{xx} u_1 + (\partial_x u_1)^2, \\ \partial_y(u_1 \partial_y u_1) &= \partial_{yy} u_1 + (\partial_y u_1)^2, \\ \partial_x(u_1 \partial_y u_2) &= u_1 \partial_{xy} u_2 + \partial_x u_1 \partial_y u_2, \end{aligned}$$

it is obtained

$$\begin{aligned} &\alpha_{11}(\partial_x u_1)^2 + \alpha_{22}(\partial_y u_1)^2 + \alpha_{22}(\partial_x u_2)^2 + \alpha_{11}(\partial_y u_2)^2 + 2\alpha_{12}(\partial_x u_1 \partial_y u_2 + \partial_y u_1 \partial_x u_2) \\ &= -\alpha_{11} u_1 \partial_{xx} u_1 - \alpha_{22} u_1 \partial_{yy} u_1 - \alpha_{22} u_2 \partial_{xx} u_2 - \alpha_{11} u_2 \partial_{yy} u_2 - 2\alpha_{12}(u_1 \partial_{xy} u_2 + u_2 \partial_{xy} u_1) \\ &+ \operatorname{div}(\alpha_{11} u_1 \partial_x u_1 + \alpha_{22} u_2 \partial_x u_2 - 2\alpha_{12}(u_1 \partial_y u_2 + u_2 \partial_y u_1), \alpha_{22} u_1 \partial_y u_1 + \alpha_{11} u_2 \partial_y u_2) \\ &= -u_1 \partial_{tt} u_1 - u_2 \partial_{tt} u_2 \\ &+ \operatorname{div}(\alpha_{11} u_1 \partial_x u_1 + \alpha_{22} u_2 \partial_x u_2 - 2\alpha_{12}(u_1 \partial_y u_2 + u_2 \partial_y u_1), \alpha_{22} u_1 \partial_y u_1 + \alpha_{11} u_2 \partial_y u_2). \end{aligned}$$

Then, considering the integral over the rectangle R and from the divergence theorem, formula (49) is achieved. \square

Theorem 14. If the initial conditions (8), $u_0(x, y)$, $v_0(x, y)$, $w_0(x, y)$, $z_0(x, y)$, have compact support contained in an open set Ω such that $\Omega \subset R$, then, the discrete energies E_h of Theorem 4 in Section 3.1 and of Theorem 8 in Section 3.2, are approximations of the continuous energy E (10), of second and fourth order respectively, that is

$$E(0) - E_h(0) = O(h^p), \tag{50}$$

where $p = 2$ for second order spatial discretization and $p = 4$ for the fourth order discretization.

Proof. The result is obtained by using Lemmas 12, 13 and taking into account that (12) is an approximation of order p of $[\partial_{tt} u_1, \partial_{tt} u_2]^T$, with $p = 2$ when the spatial discretization of Section 3.1 is considered and $p = 4$ when the spatial discretization of Section 3.2 is used. \square

4. Time discretization

Denoting $\mathbf{v}_{n,h} = \frac{d}{dt} \mathbf{u}_{n,h}$, for $n = 1, 2$, we rewrite the problem (12) as a first order system,

$$\frac{d}{dt} \begin{bmatrix} \mathbf{u}_{1,h} \\ \mathbf{u}_{2,h} \\ \mathbf{v}_{1,h} \\ \mathbf{v}_{2,h} \end{bmatrix} = \begin{bmatrix} 0 & I \\ A & 0 \end{bmatrix} \begin{bmatrix} \mathbf{u}_{1,h} \\ \mathbf{u}_{2,h} \\ \mathbf{v}_{1,h} \\ \mathbf{v}_{2,h} \end{bmatrix}, \tag{51}$$

where I is the identity matrix of dimension $2(N + 1)(M + 1)$. We notice system (51) is a Hamiltonian problem.

4.1. Exponential splitting method

We propose to approximate the exact solution of (51),

$$\begin{bmatrix} \mathbf{u}_1(t+k) \\ \mathbf{u}_2(t+k) \\ \mathbf{v}_1(t+k) \\ \mathbf{v}_2(t+k) \end{bmatrix} = \exp\left(k \begin{bmatrix} 0 & I \\ A & 0 \end{bmatrix}\right) \begin{bmatrix} \mathbf{u}_1(t) \\ \mathbf{u}_2(t) \\ \mathbf{v}_1(t) \\ \mathbf{v}_2(t) \end{bmatrix}, \quad t \geq 0,$$

being k the time step, by using an exponential splitting method as time integrator. We split the matrix of the problem (51) into two parts

$$\begin{bmatrix} 0 & I \\ A & 0 \end{bmatrix} = \begin{bmatrix} 0 & I \\ 0 & 0 \end{bmatrix} + \begin{bmatrix} 0 & 0 \\ A & 0 \end{bmatrix} = M_1 + M_2.$$

The intermediate problems

$$\frac{d}{dt} \begin{bmatrix} \mathbf{u}_{1,h} \\ \mathbf{u}_{2,h} \\ \mathbf{v}_{1,h} \\ \mathbf{v}_{2,h} \end{bmatrix} = M_i \begin{bmatrix} \mathbf{u}_{1,h} \\ \mathbf{u}_{2,h} \\ \mathbf{v}_{1,h} \\ \mathbf{v}_{2,h} \end{bmatrix}, \quad i = 1, 2,$$

can be solved exactly using that $M_i^2 = 0$ for $i = 1, 2$ and,

$$\exp(kM_1) = \begin{bmatrix} I & kI \\ 0 & I \end{bmatrix}, \quad \exp(kM_2) = \begin{bmatrix} I & 0 \\ kA & I \end{bmatrix}.$$

Then, the flows of these intermediate problems applied to $[\mathbf{u}_1, \mathbf{u}_2, \mathbf{v}_1, \mathbf{v}_2]^T$ are

$$\begin{aligned} \psi_k^{[1]} : \exp(kM_1) \begin{bmatrix} \mathbf{u}_1 \\ \mathbf{u}_2 \\ \mathbf{v}_1 \\ \mathbf{v}_2 \end{bmatrix} &= \begin{bmatrix} \mathbf{u}_1 + k\mathbf{v}_1 \\ \mathbf{u}_2 + k\mathbf{v}_2 \\ \mathbf{v}_1 \\ \mathbf{v}_2 \end{bmatrix}, \\ \psi_k^{[2]} : \exp(kM_2) \begin{bmatrix} \mathbf{u}_1 \\ \mathbf{u}_2 \\ \mathbf{v}_1 \\ \mathbf{v}_2 \end{bmatrix} &= \begin{bmatrix} \mathbf{u}_1 \\ \mathbf{u}_2 \\ \mathbf{v}_1 + \frac{k}{h^2}(A_1\mathbf{u}_1 + A_2\mathbf{u}_2) \\ \mathbf{v}_2 + \frac{k}{h^2}(A_2\mathbf{u}_1 + A_3\mathbf{u}_2) \end{bmatrix}. \end{aligned}$$

Once we have solved exactly each intermediate problem, to advance a step of size k in time, it is necessary to combine these solutions to obtain an approximation of the solution of the problem (51). To do this, first we use the symmetric second order Strang splittingting $S^{[2]}$

$$S_k^{[2]} = \psi_{k/2}^{[1]} \circ \psi_k^{[2]} \circ \psi_{k/2}^{[1]}, \tag{52}$$

and then, by composition of $S^{[2]}$, we consider the symmetric fourth order integrator $S^{[4]}$ [22,23]

$$S_k^{[4]} = S_{\alpha k}^{[2]} \circ S_{\beta k}^{[2]} \circ S_{\alpha k}^{[2]}, \quad \text{with } \alpha = \frac{1}{2 - 2^{1/3}}, \quad \beta = 1 - 2\alpha. \tag{53}$$

In (53) it is possible to save some computational cost by joining together the last step in the composition of $S_{\alpha k}^{[2]}$ and the first one in $S_{\beta k}^{[2]}$ and similarly, the last one in the composition of $S_{\beta k}^{[2]}$ and the first one in $S_{\alpha k}^{[2]}$. That is,

$$\begin{aligned} S_k^{[4]} &= \psi_{\alpha k/2}^{[1]} \circ \psi_{\alpha k}^{[2]} \circ \psi_{\alpha k/2}^{[1]} \circ \psi_{\beta k/2}^{[1]} \circ \psi_{\beta k}^{[2]} \circ \psi_{\beta k/2}^{[1]} \circ \psi_{\alpha k/2}^{[1]} \circ \psi_{\alpha k}^{[2]} \circ \psi_{\alpha k/2}^{[1]} \\ &= \psi_{\alpha k/2}^{[1]} \circ \psi_{\alpha k}^{[2]} \circ \psi_{(\alpha+\beta)k/2}^{[1]} \circ \psi_{\beta k}^{[2]} \circ \psi_{(\alpha+\beta)k/2}^{[1]} \circ \psi_{\alpha k}^{[2]} \circ \psi_{\alpha k/2}^{[1]}. \end{aligned} \tag{54}$$

Moreover, if many steps are performed without output, the last step in the composition of $S_k^{[4]}$ for one time step, can be joined with the first one for the next time step. In this way only three evaluation of $\psi^{[1]}$ and $\psi^{[2]}$ are required per time step.

The advantage of composing exact solutions in this way is that geometric properties of the true flow are preserved. Splitting methods are especially indicated for dynamical systems that possess a certain property that one wants to preserve. These methods are qualitatively superior, particularly when a long time integration is made.

These splitting methods are explicit and easy to implement. However, they are not unconditionally stable and the stability has to be studied.

4.2. Stability discussion

To study the stability of the numerical solution obtained with the schemes proposed in the previous subsection, we consider the stability interval associated to the time integrator [24].

Following a reasoning similar to the one done in [15,20], the eigenvalues of $k(-A)^{1/2}$ must be in the stability interval $[0, \omega_*]$. In [15] it was shown that ω_* in the stability interval of $S_k^{[2]}$ is 2. On the other hand, in [20] it was proved that ω_* in the stability interval of $S_k^{[4]}$ is

$$\omega_* = \sqrt{\frac{-1 + \sqrt{1 + 1152\gamma}}{48\gamma}}, \quad \gamma = \frac{6 + 5 \cdot 2^{1/3} + 4 \cdot 2^{2/3}}{36},$$

that is, $\omega_* \sim 0.9711$.

From Lemma 2, when second order finite differences of Section 3.1 are used, the stability condition is

$$\frac{k}{h} \sqrt{4(\alpha_{11} + \alpha_{22})} < \omega_*,$$

and from Lemma 6, when fourth order finite differences of Section 3.2 are used, the stability condition is

$$\frac{k}{h} \sqrt{\frac{16(\alpha_{11} + \alpha_{22})}{3}} < \omega_*.$$

Table 1 shows the ratio between the time step and the space step to reach the stability condition for the combination of the two methods of spatial discretization with the two splitting time integrators.

Table 1
Stability ratios.

	FD2 and $S_k^{[2]}$	FD2 and $S_k^{[4]}$	FD4 and $S_k^{[2]}$	FD4 and $S_k^{[4]}$
$\frac{k}{h}$	$\frac{1}{\sqrt{\alpha_{11} + \alpha_{22}}}$	$\frac{0.9711}{2\sqrt{\alpha_{11} + \alpha_{22}}}$	$\frac{\sqrt{3}}{2\sqrt{\alpha_{11} + \alpha_{22}}}$	$\frac{0.9711\sqrt{3}}{4\sqrt{\alpha_{11} + \alpha_{22}}}$

Table 2
The three cases of α_{ij} considered according to the properties of the region.

Run	λ	μ	λ/μ	ρ	α_{11}	α_{22}	$2\alpha_{12}$
1	0.5	0.25	2	1.0	1	0.25	0.75
2	0.7	0.4	1.75	0.2	7.5	2	5.5
3	0.8	0.5	1.6	1.1	1.6364	0.4545	1.1818

Table 3
Energy of second order and fourth order finite differences for run 1, run 2 and run 3.

N	$E_{h,2}(0)$	$E_{h,4}(0)$
Run 1, $E(0) = 2.234287184231071$		
50	2.228177839357746	2.234243361366416
100	2.232757751288125	2.234284409050374
200	2.233904694884349	2.234287009860595
Run 2, $E(0) = 16.980582600156140$		
50	16.934151579118957	16.980249546384506
100	16.968958909789755	16.980561508781701
200	16.977675681121259	16.980581274936370
Run 3, $E(0) = 3.737353108168337$		
50	3.727133840380259	3.737279804467453
100	3.734794783972977	3.737348466047833
200	3.736713307807078	3.737352816493909

5. Numerical experiments

In this section we consider the problem described in Section 1 with initial condition

$$u_0(x, y) = \begin{cases} \cos^3\left(\frac{5\pi}{2}r\right), & r \leq \frac{1}{5}, \\ 0, & \text{otherwise,} \end{cases}$$

being $r = \sqrt{x^2 + y^2}$. We assume $w_0(x, y) = u_0(x, y)$ and $v_0(x, y) = z_0(x, y) = 0$. We consider the computational domain $[-1/4, 1/4] \times [-1/4, 1/4]$. In this way, the initial conditions have compact support and they are of class C^2 in the computational domain.

For the numerical experiments we have used the same three cases of coefficients α_{ij} considered in [25]. Table 2 displays these coefficients.

From now on we work with $N = M$. In order to study only the error due to the spatial discretization, we compare the continuous energy (11) for the test problem, with the discrete energy

$$E_h(t)(\mathbf{u}_1, \mathbf{u}_2, \mathbf{v}_1, \mathbf{v}_2) = \frac{h^2}{2}(\mathbf{v}_1^T \mathbf{v}_1 + \mathbf{v}_2^T \mathbf{v}_2 - \begin{bmatrix} \mathbf{u}_1 \\ \mathbf{u}_2 \end{bmatrix}^T A \begin{bmatrix} \mathbf{u}_1 \\ \mathbf{u}_2 \end{bmatrix}),$$

of the semi-discrete problems at $t = 0$. We denote by $E_{h,2}(t)$ the discrete energy where matrix A is the matrix obtained in Section 3.1, when second order finite differences are used, and $E_{h,4}(t)$ the discrete energy where matrix A is the matrix obtained in Section 3.2, when fourth order finite differences are considered.

Taking into account that the function to integrate in (11) for the test problem, in polar coordinates is separable and, using integration by parts, it can be seen that

$$E(0) = \frac{\pi}{128}(9\pi^2 - 16)(\alpha_{11} + \alpha_{22}).$$

Table 3 displays the continuous energy and the discrete energies at $t = 0$ for several values of N and the three cases of coefficients α_{ij} selected.

Likewise, relative energy error for the second order finite differences and the fourth order finite differences is shown in Fig. 2 for run 2 (the graphics for run 1 and run 3 are similar). Considering the energy error due to the spatial discretization, $error_N = |E_h(0) - E(0)|$, Table 4 shows the relation between the errors when the space step is divided in a half, for second and fourth order finite differences.

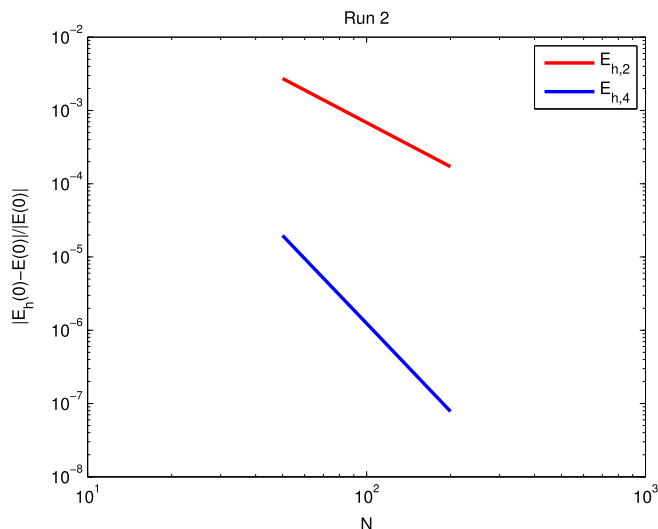


Fig. 2. Energy error for the second order finite differences and the fourth order finite differences, for run 2.

Table 4

Evolution with N of the energy error for second order and fourth order finite differences for run 2.

	$E_{h,2}(0)$	$E_{h,4}(0)$
$error_{50}/error_{100}$	3.9945	15.4554
$error_{100}/error_{200}$	3.9986	15.7176

Table 5

Stability ratios for run 1, run 2 and run 3.

Run	FD2 and $S_k^{[2]}$	FD2 and $S_k^{[4]}$	FD4 and $S_k^{[2]}$	FD4 and $S_k^{[4]}$
1	0.8944	0.4343	0.7746	0.3761
2	0.3244	0.1575	0.2810	0.1364
3	0.6916	0.3358	0.5989	0.2908

It can be appreciated, from Table 4 and the slope of the lines in Fig. 2, the spatial convergence rate for the conserved quantity $E(t)$. In this way, it can be seen numerically the second and fourth order of the discretization of Sections 3.1 and 3.2, respectively.

From Section 4, to ensure stability when the exponential splitting methods are used, k/h has to be smaller than the ratio of stability. Table 5 displays the stability ratios from Table 1, for the values of α_{ij} considered in Table 2. In Table 5, it can be seen that the stability conditions for the splitting methods are acceptable. Notice that the stability conditions for the fourth order finite differences are not much more costly than for the second order finite differences and, nevertheless, to use fourth order finite differences allows to handle spatial errors much smaller. It is good that the splitting time integrators considered are explicit and their conditions of stability are not very restrictive. Moreover, we will see that they have qualitative advantages that make them preferable to other methods.

In the following experiments only fourth order finite differences introduced in Section 3.2, the energy $E_{h,4}(t)$ and the values of α_{ij} corresponding to run 1 are used.

Because $S_k^{[2]}$ and $S_k^{[4]}$ are geometric methods, both nearly conserve the quantity $E_{h,4}(0)$. Fig. 3 displays for $N = 100$, the variation of the near conserved quantity $E_{h,4}(0) = 2.234287184231071$, for the exponential splitting integrators, $S_k^{[2]}$ with time step equal to $1/264$ and $S_k^{[4]}$ with time step equal to $1/528$.

For $N = 100$, Fig. 4 shows relative energy error $|E(0) - E_{h,4}(t)|/|E(0)|$, for the exponential splitting integrator $S_k^{[2]}$ with time steps $k = 1/264$ and $k = 1/528$ and, for the exponential splitting integrator $S_k^{[4]}$, with time step $k = 1/528$. To achieve an error of similar size, the method $S_k^{[2]}$ has to use a time step size significantly smaller than the one used by $S_k^{[4]}$.

Next, we compare the behavior of the splitting schemes and the fourth-order four-stage Runge–Kutta method.

We first show in Fig. 5, the relative energy error for the numerical solutions obtained with the fourth-order four-stage Runge–Kutta method and with $S_k^{[4]}$, both of the same order, in long time integration, for times from 0 to 100, with $N = 100$ and $k = 1/528$. It can be seen that the splitting method maintains the same size error throughout the interval of time

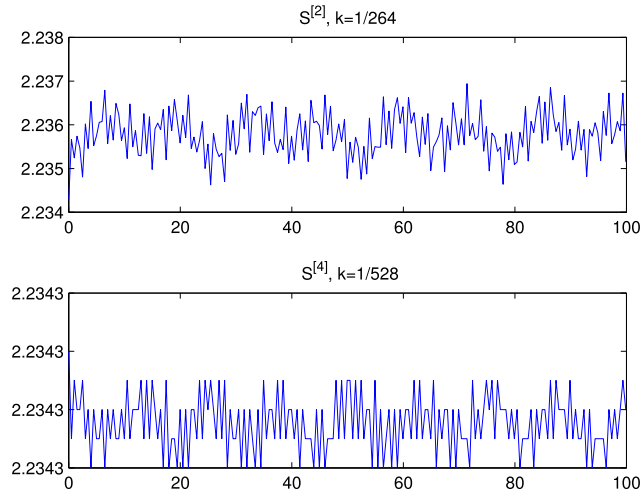


Fig. 3. Variation of the near conserved quantity $E_{h,4}(0)$ for the exponential splitting integrators, for $N = 100$ and run 1.

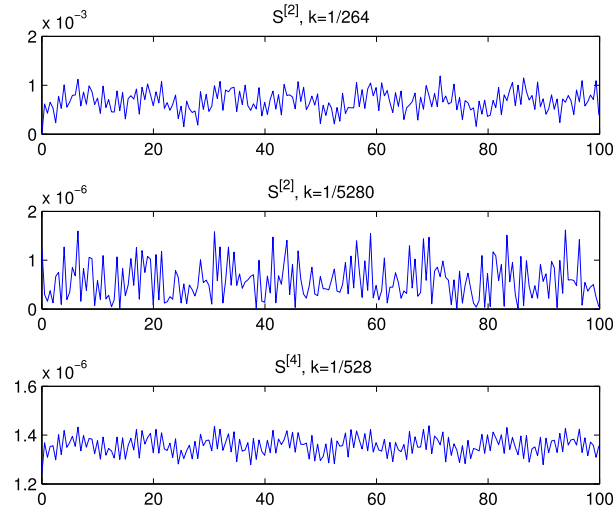


Fig. 4. Relative energy error for the exponential splitting integrators $S_k^{[2]}$ and $S_k^{[4]}$, for run 1.

$[0, 100]$, which agrees with the fact that the scheme $S_k^{[4]}$ is a geometric integrator. Whereas for the Runge–Kutta method the size of the error grows when the time increases.

Finally, we study the efficiency of the three methods considered, measuring the computational cost in terms of CPU time. For the exponential splitting integrator $S_k^{[2]}$, if the last step in the composition (52) for one step and the first one for the next step are joined together, that is, $\psi_{k/2}^{[1]} \circ \psi_{k/2}^{[1]} = \psi_k^{[1]}$, then only once of step 1 and once step 2 are needed for each step in time. Similarly, for the exponential splitting integrator $S_k^{[4]}$, if the last step in the composition (54) for one step and the first one for the next step are joined together, that is, $\psi_{\alpha k/2}^{[1]} \circ \psi_{\alpha k/2}^{[1]} = \psi_{\alpha k}^{[1]}$, then only three times of step 1 and step 2 are needed for each step in time. Then, regarding the products required for the same step size in time, for the Runge–Kutta method and $S_k^{[2]}$, the relation is four to one, for the Runge–Kutta method and $S_k^{[4]}$, the relation is four to three, and for $S_k^{[4]}$ and $S_k^{[2]}$, the relation is three to one, approximately.

We have ran the three algorithms for $N = 50$, with $k = 1/132, 1/264, 1/528$, and for $N = 100$, with $k = 1/264, 1/528, 1/1056$ and we have measured the relative energy error and the computational cost in terms of CPU time, for final time $T = 100$. We display the results in Tables 6 and 7. We notice that, for each value of N , we start using the size of time step near the stability condition for $S_k^{[2]}$. For this first time step, $S_k^{[4]}$ cannot be used, because the stability condition is not satisfied. For the third time step used with each value of N , $S_k^{[4]}$ is practically stagnant because the level of accuracy of the

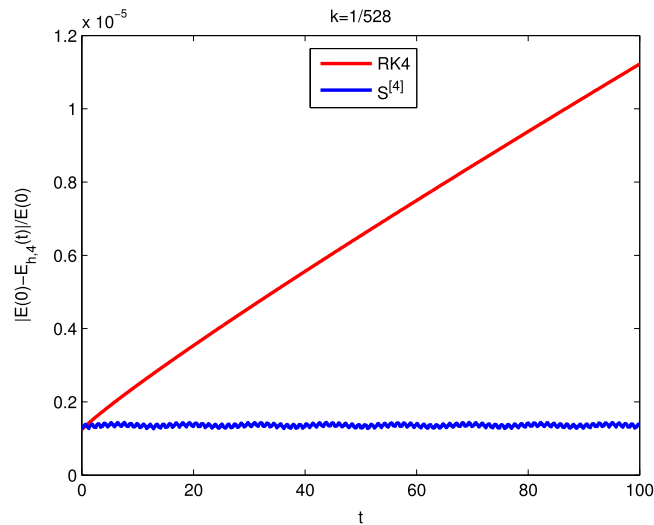


Fig. 5. Relative energy error for the exponential splitting integrator $S_k^{[4]}$ and the fourth-order four-stage Runge–Kutta method, for run 1.

Table 6
Splitting schemes, final time $T = 100$, run 1.

	$S_k^{[2]}$		$S_k^{[4]}$	
$N = 50$	Error	CPU	Error	CPU
$k = 1/132$	3.8414×10^{-3}	1.4770×10^1	–	–
$k = 1/264$	8.1342×10^{-4}	2.9310×10^1	2.1063×10^{-5}	8.7920×10^1
$k = 1/528$	1.3926×10^{-4}	5.8540×10^1	1.9707×10^{-5}	1.7669×10^2
$N = 100$	Error	CPU	Error	CPU
$k = 1/264$	3.8759×10^{-4}	1.1911×10^2	–	–
$k = 1/528$	1.2816×10^{-4}	2.3568×10^2	1.3563×10^{-6}	7.0816×10^2
$k = 1/1056$	3.1284×10^{-5}	4.7615×10^2	1.2492×10^{-6}	1.4191×10^3

Table 7
Rk4 method, final time $T = 100$, run 1.

	rk4	
$N = 50$	Error	CPU
$k = 1/132$	6.1187×10^{-3}	6.2500×10^1
$k = 1/264$	2.6210×10^{-4}	1.2429×10^2
$k = 1/528$	2.9215×10^{-5}	2.4770×10^2
$N = 100$	Error	CPU
$k = 1/264$	2.4470×10^{-4}	5.0538×10^2
$k = 1/528$	1.1211×10^{-5}	1.0037×10^3
$k = 1/1056$	1.6659×10^{-6}	2.0088×10^3

spatial discretization is achieved. The same data can be seen in Fig. 6. It can be observed that always one splitting method is better than the Runge–Kutta method. For the same error the computational cost is smaller. Moreover, for moderate errors is more efficient the splitting method $S_k^{[2]}$, while for small errors is more efficient the splitting method $S_k^{[4]}$.

The numerical experiments confirm the good behavior in the long time integration and the efficiency of the splitting methods considered.

6. Conclusions and perspectives

In this work, we provide second and fourth order accurate in space and second and fourth order accurate in time schemes to solve numerically two-dimensional coupled seismic waves. The resulting methods are explicit and it is necessary to study their stability conditions. We calculate the relation between the time step size and the space step size in the stability limit as a function of the velocities of the P wave and the S wave, which in practice can be very different. In particular, the ratio of stability is expressed in terms of the coefficients α_{11} and α_{22} . Moreover, as the time integrators are geometric integrators,

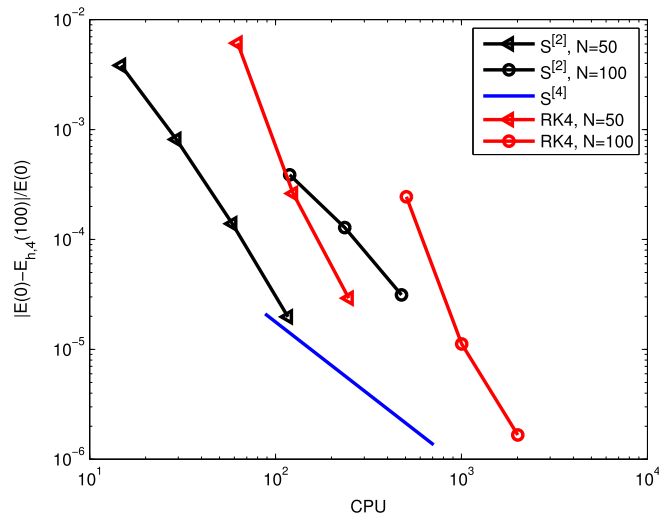


Fig. 6. Relative energy error at $T = 100$ versus CPU time for the exponential splitting integrators and the fourth-order four-stage Runge–Kutta method for run 1, for $N = 50$ and $N = 100$.

the numerical solutions have good behavior in the long time integration, in the sense that they near conserve the energy of the problem.

It remains to be studied whether the proposed methods can be used when absorbing boundary conditions are considered, as we did in [15] with similar splitting methods, for the Klein–Gordon equation with Hagstrom–Warburton absorbing boundary conditions.

Acknowledgments

The author thanks Isaías Alonso-Mallo for his comments that have helped to improve this paper.

This work has obtained financial support from project MTM2015-66837-P of Ministerio de Economía y Competitividad.

References

- [1] Y. Wencai, *Reflection Seismology: Theory, Data Processing and Interpretation*, Elsevier, 2013.
- [2] J.E. Marsden, T.J.R. Hughes, *Mathematical Foundations in Elasticity*, Dover publications, 1994.
- [3] J. Virieux, P-SV wave propagation in heterogeneous media: Velocity-stress finite-difference method, *Geophysics* 51 (1986) 889–901.
- [4] A.R. Levander, Fourth-order finite-difference P-SV seismograms, *Geophysics* 53 (1988) 1425–1436.
- [5] S. Cao, S. Greenhalgh, Finite-difference simulation of P-SV-wave propagation: a displacement-potential approach, *Geophys. J. Int.* 109 (1992) 525–535.
- [6] V.M. Cruz-Atienza, J. Virieux, Dynamic rupture simulation of non-planar faults with finite-difference approach, *Geophys. J. Int.* 158 (2004) 939–954.
- [7] S. Blanes, F. Casas, A. Murua, Splitting and composition methods in the numerical integration of differential equations, *Bol. Soc. Esp. Mat. Apl.* 45 (2008) 89–145.
- [8] R.I. McLachlan, On the numerical integration of ordinary differential equations by symmetric composition methods, *SIAM J. Sci. Comput.* 16 (1995) 151–168.
- [9] R.I. McLachlan, R. Quispel, Splitting methods, *Acta Numer.* 11 (2002) 341–434.
- [10] T.J. Bridges, S. Reich, Numerical methods for Hamiltonian PDEs, *J. Phys. A: Math. Gen.* 39 (2006) 5288–5289.
- [11] E. Hairer, G. Wanner, C. Lubich, *Geometric Numerical Integration*, Springer, 2006.
- [12] J.M. Sanz-Serna, M.P. Calvo, *Numerical Hamiltonian Problems*, Chapman and Hall, London, 1994.
- [13] Z. Wu, S. Zhang, A meshless symplectic algorithm for multi-variate hamiltonian PDEs with radial basis approximation, *Eng. Anal. Bound. Elem.* 50 (2015) 258–264.
- [14] S. Zhang, Y. Yang, H. Yang, A meshless symplectic algorithm for nonlinear wave equation using highly accurate RBFs quasi-interpolation, *Appl. Math. Comput.* 314 (2017) 110–120.
- [15] I. Alonso-Mallo, A.M. Portillo, Time exponential splitting technique for the Klein–Gordon equation with Hagstrom–Warburton high-order absorbing boundary conditions, *J. Comput. Phys.* 311 (2016) 196–212.
- [16] I. Kra, S.R. Simanca, On circulant matrices, *Notices Amer. Math. Soc.* 59 (2012) 368–377.
- [17] T. Lara, Circulant matrices, *Divulg. Mat.* 9 (1) (2001) 85–102.
- [18] B. Düring, M. Fournié, A. Rigal, High-order ADI schemes for convection–diffusion equations with mixed derivative terms, *Lect. Notes Comput. Sci. Eng.* 95 (2014) 217–226.
- [19] C. Hendricks, M. Ehrhardt, M. Günther, High-order ADI schemes for diffusion equations with mixed derivatives in the combination technique, *Appl. Numer. Math.* 101 (2016) 36–52.
- [20] A.M. Portillo, High order full discretization for anisotropic wave equations, (unpublished) results.
- [21] F. Stacey, P. Davis, *Physics of the Earth*, Cambridge University Press, 2008.
- [22] M. Suzuki, Fractal decomposition of exponential operators with applications to many-body theories and Monte Carlo simulations, *Phys. Lett. A* 146 (1990) 319–323.

- [23] H. Yoshida, Construction of higher order symplectic integrators, *Phys. Lett. A* 150 (1990) 262–268.
- [24] S. Blanes, F. Casas, A. Murua, On the linear stability of splitting methods, *Found. Comput. Math.* 8 (2008) 357–393.
- [25] J.J. Benito, F. Urea, L. Gavete, E. Saleté, A. Muelas, A GFDm with PML for seismic wave equations in heterogeneous media, *J. Comput. Appl. Math.* 252 (2013) 40–51.